Ultrahigh Brilliance Multi-MeV γ-Ray Beams from Nonlinear Relativistic Thomson Scattering

G. Sarri,[1] D. J. Corvan,[1] W. Schumaker,[2] J. M. Cole,[3] A. Di Piazza,[4] H. Ahmed,[1] C. Harvey,[1] C. H. Keitel,[4] K. Krushelnick,[2] S. P. D. Mangles,[3] Z. Najmudin,[3] D. Symes,[5] A. G. R. Thomas,[2] M. Yeung,[6] Z. Zhao,[2] and M. Zepf[1,6]

[1]*School of Mathematics and Physics, The Queen's University of Belfast, BT7 1NN Belfast, United Kingdom*

[2]*Center for Ultrafast Optical Science, University of Michigan, Ann Arbor, Michigan 48109-2099, USA*

[3]*The John Adams Institute for Accelerator Science, Imperial College of Science, Technology and Medicine, London SW7 2AZ, United Kingdom*

[4]*Max-Planck-Institut für Kernphysik, Saupfercheckweg 1, 69117 Heidelberg, Germany*

[5]*Central Laser Facility, Rutherford Appleton Laboratory, Didcot, Oxfordshire OX11 0QX, United Kingdom*

[6]*Helmholtz Institute Jena, Fröbelstieg 3, 07743 Jena, Germany*

(Received 28 July 2014; published 25 November 2014)

We report on the generation of a narrow divergence ($\theta_\gamma < 2.5$ mrad), multi-MeV ($E_{\max} \approx 18$ MeV) and ultrahigh peak brilliance ($> 1.8 \times 10^{20}$ photons s^{-1} mm^{-2} $mrad^{-2}$ 0.1% BW) γ-ray beam from the scattering of an ultrarelativistic laser-wakefield accelerated electron beam in the field of a relativistically intense laser (dimensionless amplitude $a_0 \approx 2$). The spectrum of the generated γ-ray beam is measured, with MeV resolution, seamlessly from 6 to 18 MeV, giving clear evidence of the onset of nonlinear relativistic Thomson scattering. To the best of our knowledge, this photon source has the highest peak brilliance in the multi-MeV regime ever reported in the literature.

DOI: 10.1103/PhysRevLett.113.224801 PACS numbers: 41.75.Fr, 42.65.Ky, 52.38.Ph, 52.59.Px

The generation of high-quality multi-MeV γ-ray beams is an active field of research due to the central role they play not only in fundamental research [1], but also in extremely important practical applications, which include cancer radiotherapy [2,3], active interrogation of materials [4], and radiography of dense objects [5]. As an example, giant dipole resonances of most heavy nuclei occur in an energy range of 15–30 MeV [6], exciting photofission of the nucleus.

Different mechanisms have been proposed to generate high-quality multi-MeV γ-ray beams, including bremsstrahlung emission, synchrotron emission (including the state of the art HIγS machine [1]), Compton scattering (together with its classical limit, Thomson scattering), and in-flight positron annihilation [7]. Bremsstrahlung sources are routinely used for medical applications, and exploit electron beams accelerated by linear accelerators (LINAC) [8]. Laser-driven bremsstrahlung sources, whereby the electron beam is generated via laser-wakefield acceleration (LWFA) [9] have also been recently reported [5,10,11]. However, the relatively broad divergence and source size limit the peak brightness achievable with this technique and a more promising physical mechanism has been identified in Compton scattering. Here, we denote the process as Thomson or Compton depending on if quantum effects, like photon recoil, are negligible or not [12]. We note, however, that some communities broadly use the term Compton source to refer also to sources exploiting relativistic Thomson scattering [1].

Laser-driven electron beams with energy per particle of the order of the GeV are now routinely available in the laboratory [9], allowing for the possibility of all-optical and compact Compton sources [12–16]. In the hard x-ray region (photon energies in the keV regime), the highest peak brilliance is obtained instead with free-electron lasers (10^{25} photons s^{-1} mm^{-2} $mrad^{-2}$ 0.1% BW obtained by PETRA III [17]) with betatron sources peaking at 10^{21}–10^{22} photons s^{-1} mm^{-2} $mrad^{-2}$ 0.1% BW [18,19].

Previous investigations of laser-driven Thomson scattering have mostly focused on the linear or single-photon regime, i.e., whenever the relativistically invariant dimensionless amplitude of the laser pulse is less than 1 ($a_0 < 1$, whereby $a_0 = eE_L/(m_e\omega_L c)$, with E_L and ω_L being the laser electric field and central frequency, respectively, and m_e being the electron rest mass) [20,21] and report on γ-ray energies ranging from a few hundreds of keV [20] up to 3–4 MeV [21]. Three main factors can in principle be modified in order to increase the energy of the generated photons: the electron Lorentz factor γ_e, the laser photon energy $\hbar\omega_L$, or the laser intensity a_0. The energy of the generated photons can in fact be estimated as: $E_\gamma \approx 4\gamma_e^2 \hbar\omega_L f(a_0)$, whereby $4\gamma_e^2$ accounts for the relativistic Doppler shift and $f(a_0) \approx 1$ for $a_0 \ll 1$ or $f(a_0) \approx a_0$ for $a_0 \geq 1$ [16]. a_0 here relates to the number of photons with which the electron is interacting simultaneously, implying nonlinear scattering for $a_0 > 1$. Perturbative nonlinear corrections ($a_0 < 1$) were first reported in Ref. [22].

Liu and collaborators recently reported on an increase in photon energy (up to 8–9 MeV) by frequency converting the scattering laser up to its second harmonic (thus

increasing $\hbar\omega_L$) [23]. However, using a higher laser frequency for scattering significantly reduces the laser energy available (crystal conversion efficiency into second harmonic of the order of 30%–50%), and the laser a_0 implying a modest number of generated photons ($\approx 3 \times 10^5$ photons per shot are theoretically inferred in Ref. [23]). This relatively low number can be easily understood if we consider that it would scale as $N_\gamma \propto a_0^2$ for $a_0 \ll 1$ [16]. The brilliance of this source is thus not higher than the laser-driven bremsstrahlung source [5,10,11] (see Fig. 4 for a comparison of reported brilliance for different γ-ray sources). To the best of our knowledge, only one work has reported on nonlinear laser-driven scattering ($a_0 \approx 1.5$) using a single laser to both drive and scatter the electrons [24]. γ-ray energies of the order of few hundreds of keV were generated but the intrinsic difficulty in scaling this system to higher energies prevents it for being used for the generation of multi-MeV γ-ray beams.

We report here on the generation of multi-MeV (maximum energy of the order of 16–18 MeV) and ultrahigh brightness ($> 10^7$ photons per shot with energy exceeding 6 MeV, implying a brightness exceeding 10^{20} photons $\mathrm{s}^{-1}\,\mathrm{mm}^{-2}\,\mathrm{mrad}^{-2}$ 0.1% BW at 15 MeV) γ-ray beams following nonlinear relativistic Thomson scattering of an ultrarelativistic laser-wakefield accelerated electron beam ($\gamma_{e^-} \approx 1100$) in the field of an ultraintense laser pulse ($a_0 \approx 2$, $\hbar\omega_L \approx 1.5$ eV). A novel γ-ray spectrometry technique allowed for the first absolutely calibrated detection of the full spectrum of the γ rays, clearly indicating onset of nonlinear effects. To the best of our knowledge, this is the γ-ray source with the highest peak brilliance in the multi-MeV energy range ever generated in a laboratory.

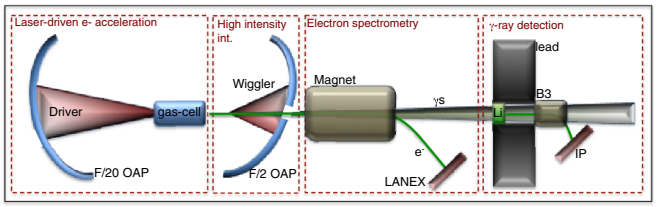

FIG. 1 (color online). Sketch of the experimental setup: a powerful laser pulse (Driver) is focussed by an $F/20$ OAP at the edge of a gas cell to generate an ultrarelativistic electron beam (first box: Laser-driven e-acceleration). A second laser beam (Wiggler) is focussed by a holed $F/2$ OAP counterpropagating to the electron beam (second box: High intensity int.). After interaction, the electron beam is deflected by a strong pair of magnets onto a LANEX scintillator screen (third box: Electron spectrometry) while the generated γ-ray beam propagates up to a Li-based spectrometer (fourth box: γ-ray detection). An $F/15$ hole in the $F/2$ OAP ensures unperturbed propagation of the scattered electron beam and generated γ-ray beam onto the detector, and minimizes backreflection of the laser in the amplification chain.

The experiment was carried out using the Astra-Gemini laser, hosted by the Rutherford Appleton laboratory [25], which delivers two laser beams each with central wavelength $\lambda_L \approx 800$ nm, pulse duration $\tau_L \approx (42 \pm 4)$ fs, and energy after compression of 18 J. Both lasers are generated from the same oscillator, avoiding problems of jitter in their synchronization. One of the two laser beams was focussed, using an $F/20$ off-axis parabola (OAP), down to a focal spot with full width half maximum of 27 ± 3 μm containing approximately 70% of the laser energy (resulting intensity $I_{\mathrm{Driver}} \approx 4 \times 10^{19}$ W/cm^2) at the edge of a 10 mm long single-stage gas cell filled with a mixture of He and N_2 (97%–3%) at a pressure of 400 mbar. Once fully ionized, this pressure corresponds to an electron background density of $(3.2 \pm 0.2) \times 10^{18}$ cm^{-3} or, analogously, to a plasma period of the order of $\tau_{\mathrm{pl}} \approx (60 \pm 2)$ fs, as measured via optical interferometry. This interaction produced, via laser-wakefield acceleration [9], a quasimonoenergetic electron beam with peak energy $E_{e^-} \approx 550$ MeV (Lorentz factor $\gamma_{e^-} \approx 1.1 \times 10^3$), and a low energy tail, with a measured divergence of the order of 2 mrad [16 ± 3 pC or $N_e = (1.0 \pm 0.2) \times 10^8$ electrons in a ± 50 MeV bandwidth around the electron peak energy, see Figs. 2(a) and 2(b) for typical electron spectra]. For each run, the shot-to-shot fluctuation in electron beam energy and charge was consistently below 10%. The shot-to-shot pointing fluctuation of the electrons was measured to occur with a standard deviation of the order of 0.7 mrad [26] and pulse front tilt effects on the electron beam axis (as first reported in Ref. [27]) were carefully minimized prior to the experimental run [26]. The second laser beam was instead focused, using an $F/2$ OAP with an $F/15$ hole in the middle, 1 cm downstream of the exit of the gas cell. At this point the electron beam diameter is measured to be (30 ± 3) μm). Insertion of a random spatial diffuser prior to the parabola allowed matching the electron beam transverse size with the high intensity focus of the laser with a peak dimensionless amplitude $a_0 = 2$ [see Fig. 2(c)]. A peaked region with $a_0 = 10$ is also present (FWHM ≈ 3 μm). However, due to its small spatial extent, only 1/100 of

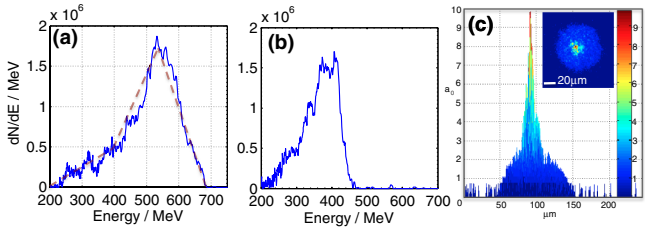

FIG. 2 (color online). (a),(b) Electron spectra used for the first and second series of experiments, respectively. In frame (a), the dashed red line represents the approximated electron spectrum used as an input for the theoretical calculations. (c) Measured intensity distribution of the laser used for scattering (Wiggler in Fig. 1).

the electrons effectively interact with this higher intensity region. Numerical calculations (discussed in the following) indicate the contribution of this interaction to the γ-ray spectrum to be negligible, and we will thus neglect it hereafter. The $F/15$ hole in the parabola was necessary in order to allow for clean transmission of the scattered electrons and the generated γ-ray beam and to avoid backreflection of the two laser beams into the amplification chain.

Downstream of the $F/2$ OAP, a pair of permanent magnets ($B = 1$ T, length of 15 cm) deflected the electrons away from the generated γ-ray beam to a LANEX [28] scintillator. This arrangement allowed resolving electron energies from 120 MeV to 2 GeV. The LANEX scintillator was cross-calibrated using absolutely calibrated imaging plates [29]. An estimate of the quantum nonlinearity parameter $\chi_0 = 5.9 \times 10^{-2} E_{e^-}[\mathrm{GeV}]\sqrt{I_L[10^{20}\ \mathrm{W/cm^2}]}$ [12] shows that in our experiment ($E_{e^-} \sim 550$ MeV and $I_L \sim 8 \times 10^{18}$ W/cm^2) quantum effects are negligible ($\chi_0 \simeq 0.01$). Moreover, by estimating the average energy $\mathcal{E}_{e^-}$ emitted by an electron with an energy of 550 MeV from the Larmor formula [30], we obtain $\mathcal{E}_{e^-} \sim 11$ MeV such that radiation-reaction effects are also negligibly small. The electron spectrum after the interaction is substantially unchanged (recoil-less interaction) and it can thus be used as a valid approximation for the initial electron spectrum.

Spatial overlap between the two laser pulses was achieved with 5 μm precision using an alignment wire whereas temporal synchronization was obtained using a spectral interferometry technique [31].

The γ rays were then spectrally resolved 2 meters downstream of the interaction. A 2 cm thick block of Li (transverse size of 5 mm) was inserted into the γ-ray beam path to allow for the generation of secondary electrons via Compton scattering. This angular acceptance was explicitly chosen to be comparable to the theoretically predicted angular spread of the γ-ray photons: $\theta_\gamma \approx a_0/\gamma_{e^-} \approx 2$ mrad. The on-axis scattered electron population retains the spectral shape of the γ-ray beam with an energy resolution of the order of the MeV. A 0.3 T, 5 cm long pair of magnets spectrally dispersed the secondary electron beam onto an absolutely calibrated imaging plate [29]. This spectrometer was encased in a 30 cm thick box of lead to minimize noise arising from off-axis scattered electrons and photons and from bremsstrahlung photons emerging from the dumping of the primary electron beam. Typical spectral resolution, as resulting from the interplay of the magnetic spectrometer resolution and uncertainty introduced by the deconvolution process, was of the order of 10%–15% whereas the uncertainty in yield was of the order of 10%. This system allowed us for the first time to measure the absolutely calibrated spectrum of the generated γ-ray beam, in an energy window between 6 and 20 MeV and an energy resolution of the order of 1 MeV (see Ref. [32] for a detailed description of this spectrometer).

In this Letter, we discuss the experimental results obtained in two different runs with the same measured intensity profile of the laser intensity at best focus [Fig. 2(c)]. In the first run, we generated a reproducible electron beam with a typical spectrum depicted in Fig. 2(a). This run produced the γ-ray spectra shown in Figs. 3(a) and 3(b). In conditions of best overlap and synchronization between the electron beam and the laser pulse, this run produced a γ-ray beam with a monotonically decreasing spectrum, with a typical number of photons per MeV exceeding 10^6, extending up to 15–18 MeV [green band in Fig. 3(a)]. The number and peak energy of the measured

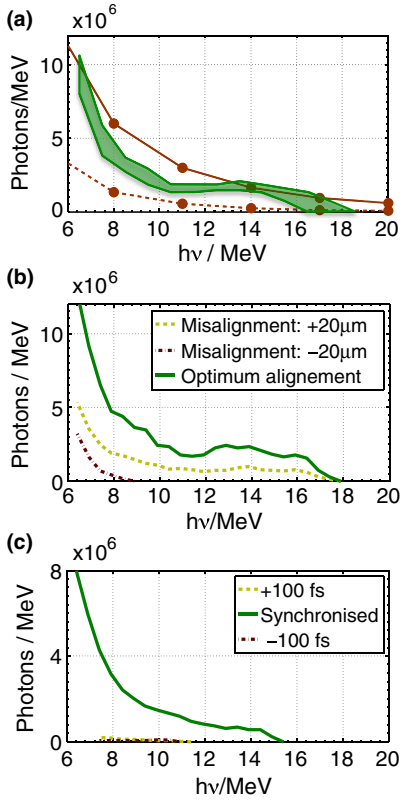

FIG. 3 (color online). (a) Green band: γ-ray spectrum as measured during the interaction of the laser-driven electron beam [spectrum depicted in Fig. 2(a)] with the high-intensity focal spot of a secondary laser beam [spatial distribution shown in Fig. 2(c)]. The band represents the uncertainty associated with the experiment, as mainly resulting from the spectral resolution of the γ-ray spectrometer and the response of the detector. Solid and dashed brown lines depict theoretical expectations for the same electron and laser parameter as the experimental ones but with $a_0 = 2$ and $a_0 = 1$, respectively. (b) The green line represents the measured spectrum for optimized electron-laser overlap [same as green band in frame (a)], whereas dashed curves depict the measured spectra if an artificial misalignment of ± 20 μm is introduced. (c) The green line represents the measured spectrum for optimized electron-laser synchronization [for an electron spectrum as the one in Fig. 2(b)] whereas dashed curves depict the measured spectra if an artificial desynchronization of ± 100 fs is introduced.

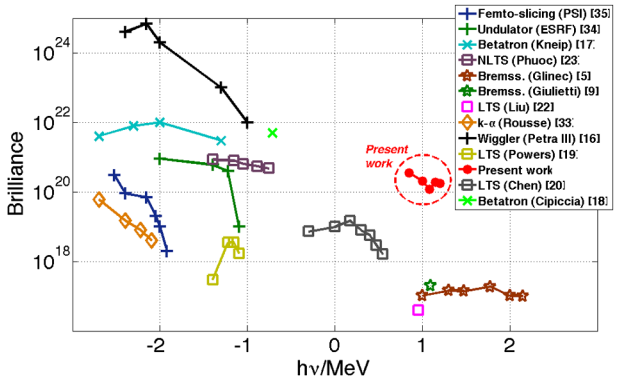

FIG. 4 (color online). Comparison of the present γ-ray source (solid red circles) with other generation mechanisms reported in the literature: free-electron laser (PETRA III, black crosses, [17]), k-α (orange diamonds, [34]), solid-state undulators (ESRF, green crosses [35] and PSI, blue crosses [36]), betatron radiation (light blue crosses [18] and light green crosses [19]), bremsstrahlung radiation (green stars [10] and brown stars [5]), nonlinear relativistic Thomson scattering (NLTS, dark purple squares [24]), and linear relativistic Thomson scattering (LTS, yellow squares [20], grey squares [21], and light purple square [23]). Brilliance is expressed in units of photons $\mathrm{s}^{-1}\,\mathrm{mm}^{-2}\,\mathrm{mrad}^{-2}$ 0.1% BW.

γ-ray photons are in good agreement with synchrotron calculations for $a_0 = 2$ [see Fig. 3(a)]. An induced spatial misalignment of $\pm 20\ \mu$m significantly reduces the signal while roughly preserving the same spectral shape [Fig. 3(b)]. No signal can be recorded if the misalignment is increased to $\pm 40\ \mu$m.

Instead, in the second run the spectrum of the laser-accelerated electron beam was as the one shown in Fig. 2(b) and this run produced the γ-ray spectra shown in Fig. 3(c). This run was used to test the γ-ray yield out of electron-laser synchronization. Changing the relative delay of the lasers by ± 100 fs reduces the signal virtually to zero [Fig. 3(c)]. It is thus clear that the observed γ-ray beam exclusively results from the electrons wiggling in the laser field.

The theoretical emission spectra have been obtained by numerically integrating the classical Lorentz equation in the presence of a plane wave laser field with a Gaussian temporal profile and an initial electron spectrum as the one depicted by the red dashed line in Fig. 2(a). Indeed, the parameters characterizing the laser field and the electron beam in the experiment are such that the plane wave approximation works reasonably well and that both quantum and radiation-reaction effects can be neglected [12]. Once the electron trajectories are determined, they have been used to calculate the radiated electromagnetic fields via the Liénard-Wiechert potential [30]. Finally, the obtained angular-resolved energy spectra have been integrated with respect to the emission angles according to the experimental condition (half-cone angle from 0 to 1.25 mrad). This procedure has been carried out for $a_0 = 1$ and $a_0 = 2$ [dashed and solid brown lines in Fig. 3(a)]. It is interesting to note that in a linear regime [$a_0 = 1$, see Fig. 3(a)] the same setup would ensure a much lower peak energy and number of photons, clearly confirming the better performance of nonlinear scattering for the generation of high brilliance and high energy γ-ray beams.

Let us now proceed to estimate the peak brilliance of our source. The source size is comparable to the electron beam diameter at interaction [$D_\gamma \approx (30 \pm 3)\ \mu$m], whereas un upper limit for divergence of the measured photon beam is given by the angular acceptance of the γ-ray spectrometer (2.5 mrad). Finally, the temporal duration would be comparable to that of the electron beam and, therefore, of the order of a half plasma period in the acceleration stage [33] [$\approx$30 fs for a plasma period of $\tau_{\mathrm{pl}} \approx (60 \pm 2)$ fs]. In a 0.1% bandwidth around 15 MeV we have approximately $(3.0 \pm 0.2) \times 10^4$ photons, implying a lower limit for the peak brilliance of $(1.8 \pm 0.4) \times 10^{20}$ photons $\mathrm{s}^{-1}\,\mathrm{mm}^{-2}\,\mathrm{mrad}^{-2}$ 0.1% BW. This brilliance is the highest ever achieved in a laboratory for multi-MeV γ-ray sources, exceeding by several orders of magnitude that achieved by bremsstrahlung sources (see Fig. 4). This is due to the unique combination of high photon energy (maximum of 15–18 MeV compared to a sub-MeV for betatron and a maximum of a few MeV for linear relativistic Thomson scattering sources), high photon number (approximately 10^7 photons with energy exceeding 6 MeV per laser shot), small divergence and source size (2.5 mrad and 30 μm compared to tens of mrad and hundreds of microns for typical bremsstrahlung sources, respectively), and short duration (tens of fs, compared to picoseconds or nanoseconds for solid-state systems).

In conclusion, we report on experimental evidence of nonlinear relativistic Thomson scattering in a two-laser counterpropagating geometry. The absolutely calibrated spectrum of the generated γ-ray beam has been seamlessly measured, with MeV resolution, from 6 to 20 MeV and provides clear experimental evidence of nonlinear relativistic Thomson scattering. Thanks to the high photon number generated, short duration, narrow divergence, and small source size, this photon source presents the highest peak brilliance ever obtained in the laboratory in a multi-MeV energy window.

G. S. and M. Z. wish to acknowledge the EPSRC Grants No. EP/L013975/1 and No. EP/I029206/1 and the technical support from the Central Laser Facility staff. J. M. C., S. P. D. M., and Z. N. wish to acknowledge the STFC Grant No. ST/J002062/1. A. G. R. T. and K. K. wish to acknowledge support from the NSF CAREER Grant No. 1054164.

[1] Y. K. Wu, *Overview of High Intensity Gamma-ray Source-Capabilities and Future Upgrades*, 2013 International

Workshop on Polarized Sources, Targets and Polarimetry (University of Virginia, 2013).
[2] A. Laugier, *ACRIM 1995, Annuaire de la Cancrologie/ Radiothrapie et des Imageries Médicales en France* (Hopital Tenon, Paris 20, 1995).
[3] T. S. Lawrence, R. K. Ten Haken, and A. Giaccia, *Principles of Radiation Oncology*, Principles and Practice of Oncology, 8th ed. (Lippincott, Williams, and Wilkins, Philadelphia, 2008).
[4] American National Standard Minimum Performance Criteria for Active Interrogation Systems Used for Homeland Security, ANSI N42.41-2007, pp. 1–35, 2008.
[5] Y. Glinec *et al.*, Phys. Rev. Lett. **94**, 025003 (2005).
[6] G. C. Baldwin and G. S. Klaiber, Phys. Rev. **73**, 1156 (1948).
[7] P. Argan *et al.*, Nucl. Instrum. Methods Phys. Res., Sect. A **228**, 20 (1984).
[8] D. I. Thwaites and J. B. Tuohy, Phys. Med. Biol. **51**, R343 (2006).
[9] E. Esarey, C. B. Schroeder, and W. P. Leemans, Rev. Mod. Phys. **81**, 1229 (2009).
[10] A. Giulietti *et al.*, Phys. Rev. Lett. **101**, 105002 (2008).
[11] W. Schumaker *et al.*, Phys. Plasmas **21**, 056704 (2014).
[12] A. Di Piazza, C. Müller, K. Z. Hatsagortsyan, and C. H. Keitel, Rev. Mod. Phys. **84**, 1177 (2012) and references therein.
[13] L. H. Gray, Proc. R. Soc. A **128**, 361 (1930).
[14] R. H. Milburn *et al.*, Phys. Rev. Lett. **10**, 75 (1963).
[15] F. R. Arutyunian and V. A. Tumanian, Phys. Rev. Lett. **4**, 176 (1963).
[16] S. Corde, K. Ta Phuoc, G. Lambert, R. Fitour, V. Malka, A. Rousse, A. Beck, and E. Lefebvre, Rev. Mod. Phys. **85**, 1 (2013).
[17] http://flash.desy.de/.
[18] S. Kneip *et al.*, Nat. Phys. **7**, 737 (2012).
[19] S. Cipiccia *et al.*, Nat. Phys. **7**, 867 (2011).
[20] N. D. Powers, I. Ghebregziabher, G. Golovin, C. Liu, S. Chen, S. Banerjee, J. Zhang, and D. P. Umstadter, Nat. Photonics **8**, 28 (2014).
[21] S. Chen *et al.*, Phys. Rev. Lett. **110**, 155003 (2013).
[22] C. Bula *et al.*, Phys. Rev. Lett. **76**, 3116 (1996).
[23] C. Liu, G. Golovin, S. Chen, J. Zhang, B. Zhao, D. Haden, S. Banerjee, J. Silano, H. Karwowski, and D. Umstadter, Opt. Lett. **39**, 4132 (2014).
[24] K. Ta Phuoc, S. Corde, C. Thaury, V. Malka, A. Tafzi, J. P. Goddet, R. C. Shah, S. Sebban, and A. Rousse, Nat. Photonics **6**, 308 (2012).
[25] C. J. Hooker *et al.*, J. Phys. IV (Paris) **133**, 673 (2006).
[26] R. J. Garland *et al.*, arXiv:1407.6979 [Phys. Plasmas (to be published)].
[27] A. Popp *et al.*, Phys. Rev. Lett. **105**, 215001 (2010).
[28] Y. Glinec, J. Faure, A. Guemnie-Tafo, V. Malka, H. Monard, J. P. Larbre, V. De Waele, J. L. Marignier, and M. Mostafavi, Rev. Sci. Instrum. **77**, 103301 (2006).
[29] K. A. Tanaka, T. Yabuuchi, T. Sato, R. Kodama, Y. Kitagawa, T. Takahashi, T. Ikeda, Y. Honda, and S. Okuda, Rev. Sci. Instrum. **76**, 013507 (2005).
[30] J. D. Jackson, *Classical Electrodynamics*, 3rd ed. (Wiley, New York, 1998).
[31] D. J. Corvan *et al.*, Opt. Exp. (to be published).
[32] D. J. Corvan, G. Sarri, and M. Zepf, Rev. Sci. Instrum. **85**, 065119 (2014).
[33] S. P. D. Mangles *et al.*, Phys. Rev. Lett. **96**, 215001 (2006).
[34] A. Rousse, P. Audebert, J. Geindre, F. Falliès, J. Gauthier, A. Mysyrowicz, G. Grillon, and A. Antonetti, Phys. Rev. E **50**, 2200 (1994).
[35] http://www.esrf.eu/Accelerators/Performance/Brilliance.
[36] http://www.psi.ch/sls/microxas/femto; P. Beaud, S. Johnson, A. Streun, R. Abela, D. Abramsohn, D. Grolimund, F. Krasniqi, T. Schmidt, V. Schlott, and G. Ingold, Phys. Rev. Lett. **99**, 174801 (2007).